AIP | Review of Scientific Instruments

A compact proton spectrometer for measurement of the absolute DD proton spectrum from which yield and ρR are determined in thin-shell inertial-confinement-fusion implosions

M. J. Rosenberg, A. B. Zylstra, J. A. Frenje, H. G. Rinderknecht, M. Gatu Johnson, C. J. Waugh, F. H. Séguin, H. Sio, N. Sinenian, C. K. Li, R. D. Petrasso, V. Yu. Glebov, M. Hohenberger, C. Stoeckl, T. C. Sangster, C. B. Yeamans, S. LePape, A. J. Mackinnon, R. M. Bionta, B. Talison, D. T. Casey, O. L. Landen, M. J. Moran, R. A. Zacharias, J. D. Kilkenny, and A. Nikroo

Citation: Review of Scientific Instruments **85**, 103504 (2014); doi: 10.1063/1.4897193
View online: http://dx.doi.org/10.1063/1.4897193
View Table of Contents: http://scitation.aip.org/content/aip/journal/rsi/85/10?ver=pdfcov
Published by the AIP Publishing

A compact proton spectrometer for measurement of the absolute DD proton spectrum from which yield and ρR are determined in thin-shell inertial-confinement-fusion implosions

M. J. Rosenberg,[1,a)] A. B. Zylstra,[1] J. A. Frenje,[1] H. G. Rinderknecht,[1] M. Gatu Johnson,[1] C. J. Waugh,[1] F. H. Séguin,[1] H. Sio,[1] N. Sinenian,[1] C. K. Li,[1] R. D. Petrasso,[1] V. Yu. Glebov,[2] M. Hohenberger,[2] C. Stoeckl,[2] T. C. Sangster,[2] C. B. Yeamans,[3] S. LePape,[3] A. J. Mackinnon,[3] R. M. Bionta,[3] B. Talison,[3] D. T. Casey,[3] O. L. Landen,[3] M. J. Moran,[3] R. A. Zacharias,[3] J. D. Kilkenny,[4] and A. Nikroo[4]

[1]*Plasma Science and Fusion Center, Massachusetts Institute of Technology, Cambridge, Massachusetts 02139, USA*
[2]*Laboratory for Laser Energetics, University of Rochester, Rochester, New York 14623, USA*
[3]*Lawrence Livermore National Laboratory, Livermore, California 94550, USA*
[4]*General Atomics, San Diego, California 92186, USA*

(Received 5 June 2014; accepted 22 September 2014; published online 10 October 2014)

A compact, step range filter proton spectrometer has been developed for the measurement of the absolute DD proton spectrum, from which yield and areal density (ρR) are inferred for deuterium-filled thin-shell inertial confinement fusion implosions. This spectrometer, which is based on tantalum step-range filters, is sensitive to protons in the energy range 1-9 MeV and can be used to measure proton spectra at mean energies of ~1-3 MeV. It has been developed and implemented using a linear accelerator and applied to experiments at the OMEGA laser facility and the National Ignition Facility (NIF). Modeling of the proton slowing in the filters is necessary to construct the spectrum, and the yield and energy uncertainties are ±<10% in yield and ±120 keV, respectively. This spectrometer can be used for *in situ* calibration of DD-neutron yield diagnostics at the NIF. © *2014 AIP Publishing LLC*. [http://dx.doi.org/10.1063/1.4897193]

I. INTRODUCTION

Charged-particle spectroscopy is a powerful tool for diagnosing fusion yield (Y), areal density (ρR), and ion temperature (T_i) in inertial confinement fusion (ICF) implosions.[1–4] Several diagnostic techniques have been used, including magnet-based spectrometers[1,5,6] and ranging filters,[7] with detection substrates consisting of image plates[8] or the solid-state nuclear track detector CR-39.[7,9–11]

Though the existing suite of charged-particle spectrometers is able to detect protons over a wide range of energies, from ~0.1 to ~30 MeV, and at a variety of incident particle fluences,[12] there are limitations to their usage that render them unavailable for certain applications. In particular, the charged particle spectrometers (CPS)[5,7] operated at the OMEGA laser facility[13] are positioned at fixed locations and are limited to proton yields above 10^8. The wedge range filter (WRF) proton spectrometers[7,14] are compact and portable, and can be fielded simultaneously at multiple positions around implosions at OMEGA and the National Ignition Facility (NIF),[15] but their energy range for proton detection is limited to 4-20 MeV. The operating parameters of existing proton spectrometers used at OMEGA and NIF, in comparison to the step range filter (SRF) proton spectrometer presented in this work, are summarized in Table I.

The SRF combines the ease-of-use advantages of the WRFs with the ability to measure proton spectra at energies as low as 1 MeV. Using steps of thin tantalum foils in front of a piece of CR-39, protons in the range of 1-9 MeV can be detected. For low-energy (~1-3 MeV) protons produced via the DD reaction,

$$\mathrm{D} + \mathrm{D} \rightarrow \mathrm{T}(1.01\,\mathrm{MeV}) + \mathrm{p}(3.02\,\mathrm{MeV}), \qquad (1)$$

the SRF can be used to measure the energy downshift of the proton spectrum, from which the total ρR is inferred. This detector is intended to diagnose thin-shell, deuterium-filled (D_2 or D^3He) implosions with a ρR less than 30 mg/cm^2, at which point the protons are ranged out. In addition to having utility in physics studies of shock-driven implosions,[16] these proton detectors can be used for an *in situ* calibration of DD-neutron detectors on OMEGA or NIF,[17] using a technique described by Waugh *et al.*[18]

This paper is organized as follows: Sec. II discusses the SRF detector design and principles of spectral measurement; Sec. III presents initial data obtained using a linear accelerator[19] and on the OMEGA and NIF laser facilities; Sec. IV discusses analysis uncertainties; and Sec. V presents possible applications of this detector and concluding remarks.

II. DESIGN AND ANALYSIS PRINCIPLES

The SRF detector, designed to fit into a WRF spectrometer casing, consists of a thick aluminum frame (background plate), to which are adhered steps of thin tantalum filters, followed by a piece of CR-39. Photographs of a sample SRF setup and a cartoon front view of the foils, as seen from an implosion, are shown in Figure 1. Two separate designs have

a)Electronic mail: mrosenbe@mit.edu

TABLE I. Operating parameters for the charged particle spectrometers (CPS),[5,7] wedge range filter (WRF) proton spectrometers,[7,14] and the new step range filter (SRF) proton spectrometer. CPS has a wide energy range, but is limited to two fixed positions on OMEGA. The WRFs are portable, but are limited to proton energies above 4 MeV. The SRF combines the portability of the WRF with a lower energy range. It should be noted that although the current SRF is limited to proton spectral measurements in the range of ~1–3 MeV, it is capable of detecting protons up to ~9 MeV.

Spectrometer	Facility	Location (positions)	Energy range	Yield range
Charged particle spectrometers (CPS)	OMEGA	Fixed (2)	0.1–30 MeV	$\sim 10^{8}$–10^{13}
Wedge range filter (WRF)	OMEGA	Portable (~10)	4–20 MeV	$\sim 10^{6}$–10^{11}
	NIF	Portable (~8)	4–20 MeV	$\sim 10^{7}$–10^{12}
Step range filter (SRF)	OMEGA	Portable (~10)	1–3 MeV	$\sim 10^{6}$–10^{11}
	NIF	Portable (~8)	1–3 MeV	$\sim 10^{7}$–10^{12}

been implemented to make spectral measurements at slightly different energy ranges: a thicker set of foils, with quadrants covered by nominally 10, 14, 19, and 23 μm of tantalum, and a thinner set of foils, with quadrants covered by nominally 5, 10, 15, and 20 μm of tantalum. These particular filters were chosen to optimize measurement of DD protons in the energy range ~1–3 MeV. The SRF is conceptually similar to the WRF proton spectrometers,[7,14,20] which use a continuous ramp, rather than discrete steps of different thicknesses. In each design, the aluminum background plate is 3180 μm thick to fully stop protons up to 25 MeV and to provide a region for characterization of intrinsic background in the CR-39.[21]

The proton signal measured behind the four step filters is used to infer the total proton yield and to construct a spectrum based on modeling of the energy ranging through each Ta foil. Consider an example using the thick detector package, with an incident Gaussian proton spectrum at a peak energy of $E_0 = 2.5$ MeV and a spectral width of $\sigma = 0.25$ MeV, representative of a downshifted DD-proton spectrum. Figure 2 shows this incident spectrum (black) and the resulting spectra (red) after ranging through the different Ta filters. The SRIM stopping power tables[22] were used for these calculations, as well as a zeroth order treatment of energy straggling, which further broadens the spectrum. 100% of the protons pass through the 10-μm Ta foil above the ~100 keV detection cutoff.[7] 99% are detected by the CR-39 behind the 14-μm-thick foil. The 19-μm foil permits 57% of the protons to be detected, while the 23-μm foil permits only 7% of the protons. The number of protons detected per cm^2 behind each filter, S_{10}, S_{14}, S_{19}, and S_{23}, are used to constrain the three parameters describing a Gaussian spectrum—the total yield Y, mean energy E_0, and the spectral width σ. In practice, a hypothetical incident spectrum, characterized by a total yield, mean energy, and spectral width, is selected and propagated through each of the four filters. The modeled signal generated behind each of the filters is then compared to the measured data. The SRF-inferred spectrum is the spectrum that produces optimal agreement between the modeled and measured signal behind the four filters. Thus, in contrast to the WRF, which uses information about the number and diameter of proton tracks behind a filter with a continuous range of thicknesses, the SRF infers properties of the proton spectrum simply from the number of proton tracks behind discrete filters of different thicknesses. This analysis principle using four

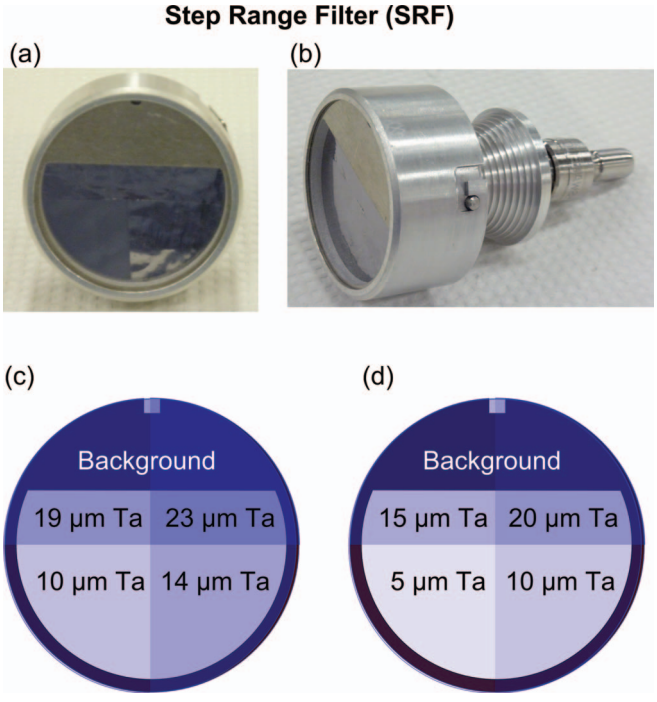

FIG. 1. (a) Front and (b) side view of a representative step range filter (SRF) setup. Two different configurations, the (c) thick and (d) thin SRF, have been developed. The thickness of the different tantalum filters is indicated. The aluminum background plate, 3180 μm thick, covers the upper ~1/3 of the module and provides a background region on the CR-39 behind the filter stack.

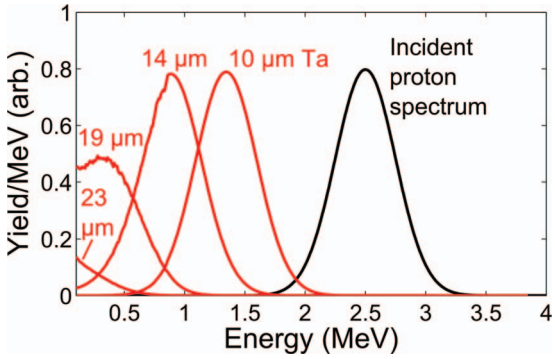

FIG. 2. Simulated proton spectra behind 10 μm, 14 μm, 19 μm, and 23 μm Ta filters (red curves). The black curve represents the incident proton spectrum, with an average energy of 2.5 MeV and a Gaussian σ of 0.25 MeV. The CR-39 detection cutoff energy is 0.1 MeV.

filters applies for any 3-parameter model spectrum, though for simplicity, the interpretation and discussion of the SRF results herein assume a Gaussian spectrum. For DD-protons around ~1-3 MeV, affected by a small energy downshift, the assumption of a Gaussian spectrum is usually valid.

III. RESULTS

The SRF proton spectrometer has been tested on the Linear Electrostatic Ion Accelerator (LEIA)[19] and used to diagnose thin-shell D_2 and D^3He-filled implosions at OMEGA and the NIF.

A. Demonstration of the SRF principle using LEIA

Initial testing of the SRF was conducted on LEIA, as depicted schematically in Figure 3.[19] LEIA generates a beam of deuterons at energies up to 150 keV, which impinges on an ErD_2 target. The resulting DD fusion reactions (Eq. (1)) produce a spectrum of protons around 3.0 MeV, which are detected by the SRF and by a surface barrier detector (SBD) that records the energy and number of individual particles. The SBD is energy-calibrated using α particles produced by the decay of ^{226}Ra. The proton energy incident on the SRF is determined by the SBD on separate LEIA experiments, with the SBD placed in the SRF position, and filtered with the appropriate additional filtering. Having an independent (SBD) measurement of the DD-p energy and yield allows for careful verification and uncertainty assessment of the SRF measurements.

Experiments on LEIA demonstrate the sensitivity of the SRF to proton spectra of different average energies. Figure 4 shows the resulting signal based on the proton fluence transmitted through each filter for a variety of incident proton spectra, ranging from $E_0 = 3.04$ MeV to $E_0 = 1.80$ MeV. The lower proton energies, measured by the SBD, are achieved by placing an additional filter in front of the SRF to range down DD protons that are born at 3.04 MeV.

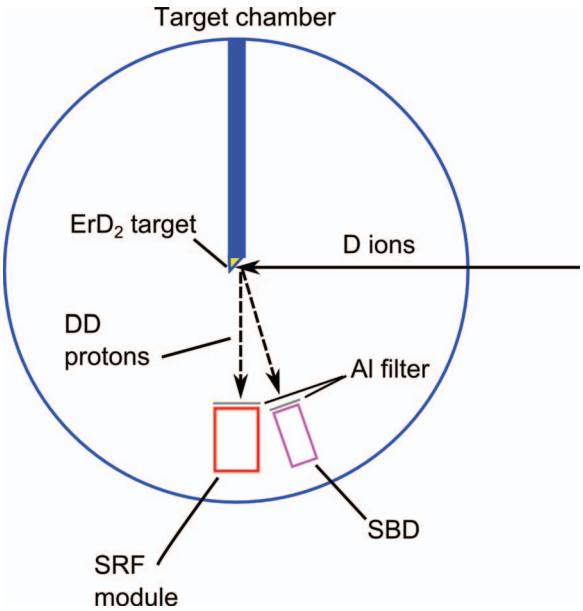

FIG. 3. Diagram of experimental setup on the Linear Electrostatic Ion Accelerator (LEIA). A deuteron beam incident on a ErD_2 target generates DD protons, which are detected by both a surface barrier detector (SBD) and the SRF. Aluminum filters are used sometimes to range down DD protons to lower energies, as discussed in the text.

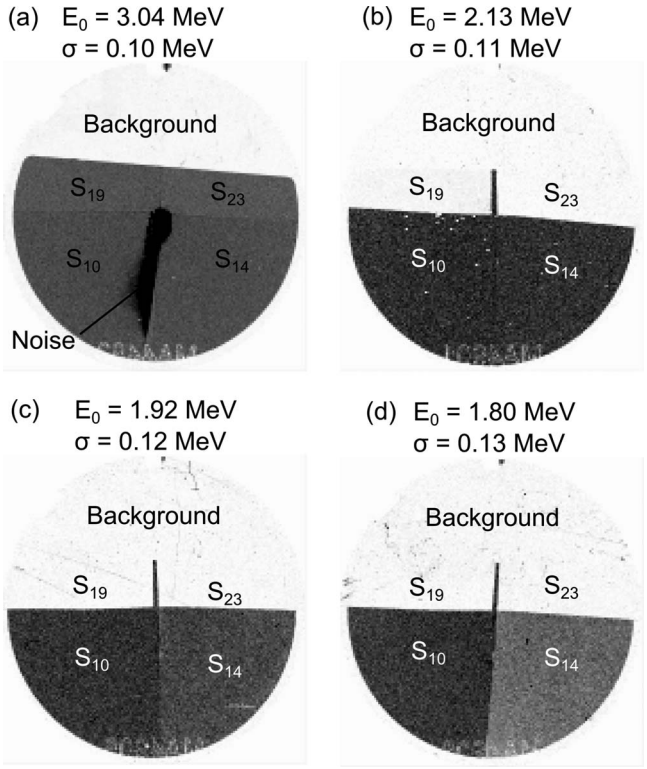

FIG. 4. SRF-measured DD-proton signal in LEIA experiments at incident mean proton energies of (a) 3.04 MeV, (b) 2.13 MeV, (c) 1.92 MeV, (d) 1.80 MeV, as determined by the SBD. Darker signifies a greater proton fluence. As the proton energy decreases, the relative signal between each window changes: S_{14}/S_{10} decreases as a larger fraction of the protons is ranged out in the 14-μm Ta filter. The relative signal ratios are presented in Table II.

At $E_0 = 3.04$ MeV (no additional filtering), nearly all protons pass through each filter and are detected on the CR-39. Only 5% fewer protons are detected behind the 19-μm and 23-μm filters than behind the 10-μm and 14-μm filters, though this measured loss of protons is only slightly outside of measurement uncertainty. Protons at the low-energy tail of the spectrum are ranged out in the thicker filters.

At $E_0 = 2.13$ MeV (~40 additional μm Al filtering), all protons are ranged out by the 23-μm filter, while 98% of protons are ranged out in the 19-μm filter. The 14-μm filter permits 98% of the protons, within measurement uncertainty of 100%, while the 10-μm filter transmits 100% of the protons.

At $E_0 = 1.92$ MeV (~45 μm additional Al filtering), no protons are detected behind the 23-μm or 19-μm filters, 88% of protons are detected behind the 14-μm filter, and 100% of the protons are detected behind the 10-μm filter.

The data using 1.80-MeV protons (~50 additional μm Al filtering) further illustrates the effects of ranging, as only 71% of protons are detected behind the 14-μm filter and 100% of the protons are detected behind the 10-μm filter. For these fairly narrow spectra, σ~0.10–0.13 MeV as measured by the SBD, the ranging out of part of the proton spectrum is

TABLE II. Measured SRF ratios of proton signal behind each of the four filters and the SRF-inferred average energy and spectral width based on modeling of spectral ranging through the different filters in LEIA experiments. The SBD-measured average energy and spectral width are shown for comparison. The difference between the SBD and SRF energy measurement helps identify uncertainties in the SRF analysis. Uncertainty in the SRF-inferred E_0 and σ represents degeneracy between those two quantities, as the two fitting parameters need to match only one proton signal ratio (the others being either 0 or ~1 and, therefore, not highly sensitive to the incident proton energy). In this case, the uncertainty in the signal ratios did not significantly contribute to the uncertainty in the SRF-inferred mean energy or linewidth, as the ±4% uncertainty in signal ratio is equivalent to a ~±0.02 MeV uncertainty in mean energy or in linewidth, which is smaller than the degeneracy-related uncertainty in either quantity. The overall difference between the SBD-measured E_0 and the SRF-inferred E_0 characterizes uncertainty in the SRF measurement, which is ~100 keV. The uncertainty estimates are discussed in more detail in Sec. IV.

SRF measured proton signal ratios			SRF E_0 (MeV)	SRF σ (MeV)	SBD E_0 (MeV)	SBD σ (MeV)
S_{14}/S_{10}	S_{19}/S_{10}	S_{23}/S_{10}				
0.99 ± 0.04	0.95 ± 0.04	0.94 ± 0.04	3.10 ± 0.05	0.10 ± 0.03	3.04	0.10
0.98 ± 0.04	0.02 ± 0.001	0	2.13 ± 0.03	0.11 ± 0.02	2.13	0.11
0.88 ± 0.04	0	0	2.04 ± 0.04	0.12 ± 0.03	1.92	0.12
0.71 ± 0.03	0	0	1.97 ± 0.03	0.13 ± 0.05	1.80	0.13

observed behind only a single filter at a time. As at most one filter transmits a non-zero, non-unity fraction of the protons, the relative signal behind each filter is a sensitive measurement of the average energy of the proton spectrum.

These data have been analyzed using the SRF analysis technique (inferring the incident proton spectra based on the measured signal ratios) to compare to the known, SBD-measured spectral parameters. By contrasting the SBD spectral measurements to the SRF data, it is possible to estimate the uncertainties in the SRF-determined incident proton energy. A summary of the SRF-inferred spectral quantities and measured proton signals, and actual, SBD-measured spectral quantities, is presented in Table II. Given an incident proton mean energy and spectral width, a model of proton ranging[22] through each of the SRF filters produces modeled proton spectra and modeled proton signal behind each filter. The model used to analyze the LEIA data includes spectral dispersion and a zeroth order treatment of energy straggling.

The uncertainties in the signal ratios (S_{14}/S_{10}, S_{19}/S_{10}, S_{23}/S_{10}) are based largely on the uncertainties in the signals measured behind each individual filter (S_{10}, S_{14}, S_{19}, S_{23}), which arise primarily from uncertainty in signal/background discrimination. Counting statistics typically contribute an uncertainty of <±1% on an individual measurement, while signal/background discrimination contributes a ~±3% uncertainty. Thus, the uncertainty on an individual measurement is ~±3% and the uncertainty on the ratio of two measurements is, therefore, typically ~±4%.

The SRF data taken on LEIA show that the analysis captures the incident proton energy as measured by the SBD to within 150 keV, and to within 50 keV at energies of 2-3 MeV. It is shown in Sec. IV that this ~100 keV error in the SRF energy measurement is roughly consistent with the energy uncertainty determined from uncertainty inherent in the modeling. Some uncertainty in the SRF-inferred energy based on the signal ratios stems from the degeneracy between E_0 and σ when matching one signal ratio. For example, in the 1.92 MeV experiment, it is only necessary to match one relative signal ratio (S_{14}/S_{10}) with two incident spectral parameters (E_0 and σ). The ranging model is able to produce $S_{14}/S_{10} = 0.88$ for several combinations of (E_0,σ) centered around (2.04, 0.12) MeV, within ±0.04 MeV for both E_0 and σ. This degeneracy issue is illustrated in Figure 5. It is a particular concern for inferring narrow spectra, as discussed further in Sec. IV.

Additionally, it is inferred from the spectral modeling that in these experiments, all protons are detected behind the 10-μm Ta filter, which means that the yield of the incident protons is simply that inferred behind the 10-μm Ta filter. Even though only one ratio is used and there is some degeneracy between E_0 and σ, the range of possible solutions is constrained by the fact that none of them allow for any fraction of the spectrum to be ranged out in the 10-μm Ta filter. For broader spectra, often observed at OMEGA and, especially, in NIF implosions, there can be multiple filters that allow through a non-zero, non-unity fraction of protons. Under these conditions, the inferred proton energy and linewidth are simultaneously constrained by multiple signal ratios. For a sufficiently low incident proton mean energy or sufficiently broad incident spectrum, a fraction of the proton spectrum may be ranged out even in the thinnest (e.g., 10-μm) Ta filter and modeling is necessary to infer the incident proton yield.

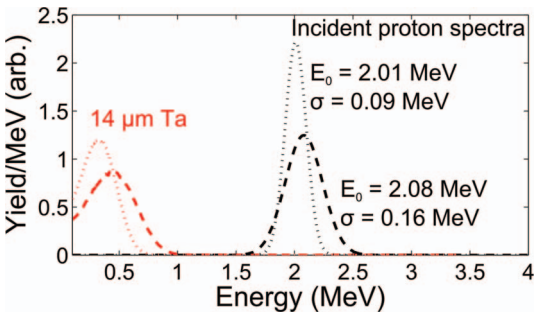

FIG. 5. Simulated proton spectra incident on the SRF (black) and transmitted through the 14 μm Ta filter (red). For both a higher-energy, broader spectrum (dashed, $E_0 = 2.08$ MeV, $\sigma = 0.16$ MeV) and a lower-energy, narrower spectrum (dotted, $E_0 = 2.01$ MeV, $\sigma = 0.09$ MeV), 88% of the protons are transmitted through the 14 μm Ta filter. Thus, there is a degeneracy in inferring both E_0 and σ from one relative signal ratio (S_{14}/S_{10}).

TABLE III. SRF- and CPS-measured DD-proton yield, mean energy, and spectral width for three D^3He-filled thin-glass-shell implosions at OMEGA. The SRF-inferred E_0 and σ are bounds, based on a combination of energy and spectral width at which at least 95% of the proton spectrum is transmitted through the 20-μm Ta filter. Though the energy lower bound is fairly rigid, if the proton spectrum had a significantly higher energy, it could also permit a wider upper-limit on the spectral width.

OMEGA shot	SRF measured proton yields				SRF E_0 (MeV)	SRF σ (MeV)	CPS Yield	CPS E_0 (MeV)	CPS σ (MeV)
	Y_5	Y_{10}	Y_{15}	Y_{20}					
70400	2.05×10^{10}	2.55×10^{10}	2.45×10^{10}	2.52×10^{10}	>2.84	<0.15	2.71×10^{10}	3.18	0.14
70561	2.74×10^{10}	3.01×10^{10}	2.61×10^{10}	2.89×10^{10}	>2.84	<0.15	3.06×10^{10}	3.10	0.13
70562	1.91×10^{10}	1.82×10^{10}	1.77×10^{10}	1.84×10^{10}	>2.84	<0.15	2.73×10^{10}	3.14	0.13

B. Use on OMEGA and NIF implosions

The SRF was also used to diagnose thin-glass-shell ICF implosions at OMEGA and the NIF. Three experiments at OMEGA used ~850-μm diameter, ~2.3–μm-thick SiO_2 shells filled with ~15 atm D^3He gas, imploded by 13.8–15.8 kJ laser energy in a ~0.6 ns laser pulse. These implosions generated $2\text{-}3\times10^{10}$ DD protons with an average energy of 3.1 MeV, which were detected by the "thin" SRF configuration at a distance of 175 cm from the implosion. At this position, the fluence was $5\text{-}8\times10^4$ protons per cm^2 at the SRF spectrometer. On these implosions, and in general, 14.7-MeV D^3He protons were not detected by the SRF, as they pass through the CR-39 at an energy above the upper limit for proton detection.

DD-proton signal images obtained on three implosions on OMEGA, shots 70400, 70561, and 70562, are shown in Figure 6. All three images show a near-uniform proton signal behind the four different filters, which were made of 5 μm, 10 μm, 15 μm, and 20 μm thick Ta. On shot 70400, the signal behind the 5-μm Ta filter shows a reduced proton signal as a result of track overlap,[23] between D^3He-α and the DD protons. On the two subsequent shots, 70561 and 70562, the data were processed in such a fashion that track overlap behind the 5-μm Ta filter was insignificant. The fact that a nearly identical fluence was observed behind each filter suggests that no significant part of the proton spectrum was ranged out in any of the filters. The incident proton mean energy and spectral width can therefore be constrained to those solutions that permit 100% of protons through the 20-μm Ta filter. Furthermore, the determination of the proton yield is straightforward, and can be computed entirely based on the measured proton signal behind any of the filters. For example, on shot 70400, the proton fluence behind the 10-μm Ta filter fluence was $S_{10} = 6.63 \times 10^4/cm^2$. With the detector at a distance of 175 cm from the implosion, the proton yield inferred behind the 10-μm Ta filter is therefore $Y_{10} = S_{10}[4\pi(175)^2] = 2.55 \times 10^{10}$, which is in reasonable agreement with a separate DD-proton yield measurement of 2.71×10^{10} (see Table III).

The inferred proton yields, mean proton energy, and linewidth are summarized in Table III. The results are compared to measurements obtained on the same shots using the CPS.[5,7] The CPS measurements are averages from two different spectrometers, CPS1 and CPS2, and as shown in Table III, the SRF-determined mean energy and linewidth agree with the CPS measurements. Differences in observed yield between different lines of sight may be due to electric and/or magnetic fields around the implosion that produce spatial anisotropies in charged fusion product fluence.[24] The CPS-measured DD-proton spectrum on shot 70561 was used as the incident spectrum on the SRF, and the spectrum behind each filter is shown in Figure 7. For the incident mean proton energy of $E_0 = 3.10$ MeV and spectral width $\sigma = 0.13$ MeV, none of the protons are ranged out by any of the filters, as concluded from the SRF data.

The "thick" SRF configuration was used to measure the DD-proton spectrum from a D_2-filled, thin-glass-shell

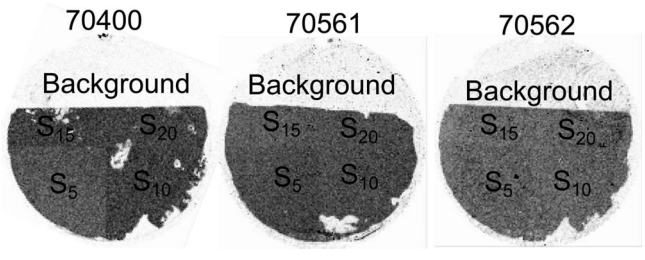

FIG. 6. DD-proton signal measured using the "thin" SRF (5, 10, 15, 20-μm Ta filters) on three D^3He-filled thin-glass-shell implosions on OMEGA (shots 70400, 70561, 70562). Dark signifies a greater proton fluence. In each experiment, the proton spectrum exiting the implosion has a mean energy ~3.1 MeV, energetic enough that the entire spectrum is transmitted through each filter. The 5-μm Ta filter also transmits D^3He-α particles, which on shot 70400 produced significant track overlap[23] and loss of ~20% of the proton signal.

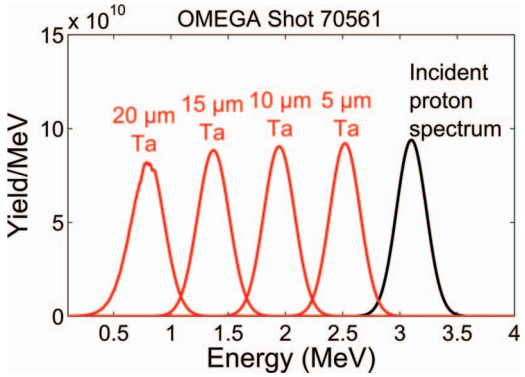

FIG. 7. CPS-measured DD-proton spectrum from OMEGA shot 70561, transmitted through each of the four filters of the "thin" SRF. The incident spectrum has a mean proton energy of $E_0 = 3.10$ MeV, with a spectral width of $\sigma = 0.13$ MeV. The resulting proton spectra (red) ranged through the 5 μm, 10 μm, 15 μm, and 20 μm Ta (thin SRF filters) are shown. 100% of the protons are transmitted through every filter, as demonstrated in the SRF measurement.

FIG. 8. DD-proton signal obtained at three different detector positions using the "thick" SRF (10, 14, 19, 23-μm Ta filters) on NIF direct-drive D_2-filled thin-glass shell shot N130129. Dark signifies a greater proton fluence. A similar absolute fluence level and ratio of proton signals is observed at each detector. The gradation in fluence across the different windows, with a finite fraction of the proton spectrum permitted behind multiple windows, indicates a fairly broad proton spectrum.

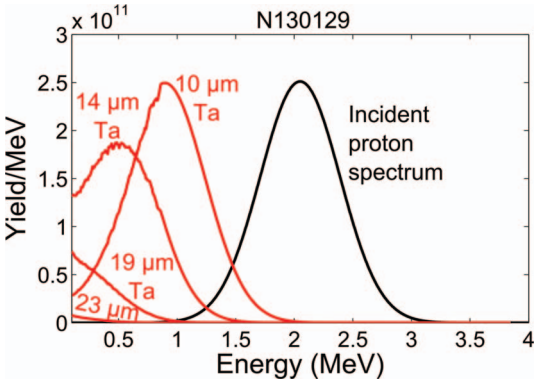

FIG. 9. SRF-inferred DD-proton spectrum from NIF shot N130129, transmitted through each of the four filters of the "thick" SRF. The incident spectrum has a mean proton energy of $E_0 = 2.05$ MeV, with a spectral width of $\sigma = 0.34$ MeV. The resulting proton spectra (red) ranged through each of 10 μm, 14 μm, 19 μm, and 23 μm Ta (thick SRF filters), above the CR-39 detection cutoff energy of 0.1 MeV, are shown. A decreasing fraction of the proton spectrum is transmitted through the increasingly thick filters.

implosion at the NIF. The experiment (shot N130129) used a 4.6-μm-thick, 1533-μm diameter SiO_2 capsule filled with 10 atm D_2 gas, which was driven by 51 kJ laser energy in a ~1.4 ns pulse in the polar-direct-drive[25,26] configuration. A DD(-neutron) yield of 2.5×10^{11} was measured by neutron time-of-flight (nTOF) detectors[27,28] and indium activation.[17] As this implosion had a total areal density of ~18 mg/cm^2, as inferred from the downshift of secondary proton spectra measured by WRF spectrometers,[3,7] the DD protons escaped the implosion and were detected by the SRF.

Three "thick" SRFs were fielded in close proximity to each other at a distance of 375 cm from the implosion; the proton fluence images are shown in Figure 8 and the raw proton yield measurements behind each filter and signal ratios are summarized in Table IV. Each SRF shows a gradually decreasing fluence of protons with increasing filter thickness. On average, the ratio of proton signal behind the 14-μm filter to that behind the 10-μm filter is $S_{14}/S_{10} = 0.71 \pm 0.02$, while $S_{19}/S_{10} = 0.13 \pm 0.01$ and $S_{23}/S_{10} = 0.014 \pm 0.002$, where here the error represents the standard deviation of the different measurements. The variation in the signal ratios from one position to the next likely reflects random uncertainty in signal/background discrimination or small differences in the Ta filter thicknesses, of order 0.2 μm. This reduction in fluence across the different filters, in contrast to sharp cutoffs in fluence demonstrated in tests at the LEIA accelerator, indicates a fairly broad DD-proton spectrum. Analysis of this data and the determination of the total proton yield, incident mean energy, and spectral width are summarized at the bottom of Table IV, with the resulting spectra shown in Figure 9.

Because three spectral parameters (total yield, mean energy, and spectral width) are fit by four measured quantities, the inferred spectrum is constrained. Based on the relative signal ratios of $S_{14}/S_{10} = 0.71$, $S_{19}/S_{10} = 0.13$, and $S_{23}/S_{10} = 0.014$, a mean incident proton energy of $E_0 = 2.05$ MeV and a spectral width of $\sigma = 0.34$ MeV are inferred. The resulting simulated signal ratios of $S_{14}/S_{10} = 0.71$, $S_{19}/S_{10} = 0.13$, and $S_{23}/S_{10} = 0.008$ are in good agreement with the measured values, to within uncertainties in proton signal measurement and spectral modeling. The remaining discrepancy between the measured and modeled S_{23}/S_{10} ratios may be attributed to errors in the proton straggling model at low proton energy, which is only a concern at very low signal ratios (i.e., when most of the detected protons are at very low energy). The variation in inferred spectral quantities based on the signal ratios at each position are only ±1.5% in yield, ±0.02 MeV in mean energy and ±0.03 MeV in linewidth; as will be shown in Sec. IV, this variation is of similar magnitude to the measurement uncertainty, providing confidence in the uncertainty calculation. For the N130129 measurement, the mean proton energy in particular is well-constrained, as deviations in energy up to only 0.04 MeV are permitted before an additional deviation of 10% in the relative proton signal is produced, larger than the measured yield uncertainty. Based on the proton energy downshift in the implosion, to 2.05 MeV, from the birth DD-proton energy of 3.02 MeV, a total ρR of 13 ± 3 mg/cm^2

TABLE IV. SRF-measured proton yields through each of the 10-μm, 14-μm, 19-μm, and 23-μm Ta filters, and ratios of proton signal behind each of the four windows, on NIF shot N130129. The measured signal ratios have baseline uncertainties of ±4%, as previously discussed. The average values are used to infer the incident DD-proton yield, mean energy, and spectral width (see Figure 9).

Detector	SRF measured proton yields				SRF signal ratios					
Position	Y_{10}	Y_{14}	Y_{19}	Y_{23}	S_{14}/S_{10}	S_{19}/S_{10}	S_{23}/S_{10}	SRF inferred		
Position 1	1.78×10^{11}	1.22×10^{11}	2.42×10^{10}	2.85×10^{9}	0.69	0.14	0.016			
Position 2	2.02×10^{11}	1.49×10^{11}	2.52×10^{10}	2.34×10^{9}	0.74	0.13	0.012	Yield	E_0 (MeV)	σ (MeV)
Position 4	2.17×10^{11}	1.53×10^{11}	2.98×10^{10}	3.18×10^{9}	0.71	0.14	0.015			
Average	1.99×10^{11}	1.41×10^{11}	2.64×10^{10}	2.79×10^{9}	0.71	0.13	0.014	2.07×10^{11}	2.05	0.34

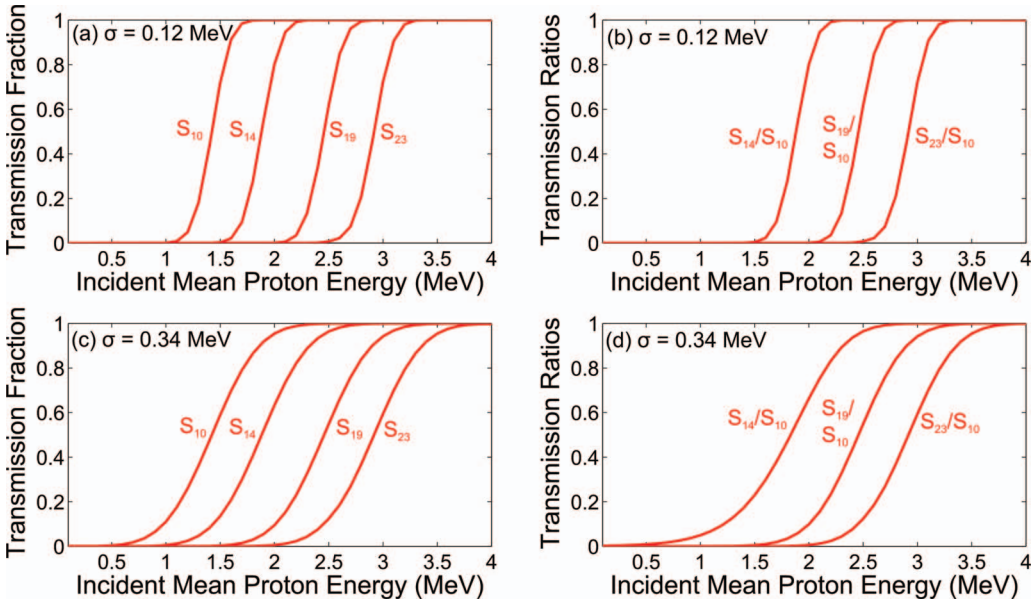

FIG. 10. (a),(c) Fraction of protons transmitted through thick SRF filters (10 μm, 14 μm, 19 μm, and 23 μm Ta) and (b),(d) ratio of protons transmitted through the filters as a function of incident mean proton energy, for $\sigma = 0.12$ MeV (top) and $\sigma = 0.34$ MeV (bottom). A decreasing fraction of the proton spectrum is transmitted through the increasingly thick filters.

is inferred, in agreement with the measured total ρR from the downshift of secondary D^3He protons, 18 ± 5 mg/cm^2. Thus, the SRF proton spectrometer can be used as a ρR diagnostic on implosions with deuterium fuel and sufficiently low ρR (<30 mg/cm^2).

IV. DISCUSSION OF APPLICABILITY AND UNCERTAINTIES

Experiments at the accelerator-based DD-p source (LEIA) and at OMEGA and the NIF demonstrate the utility of the SRF for determination of the DD proton spectrum in the energy range of ~1–3 MeV. These data also help identify uncertainties in the inference of proton yield, the mean proton energy, and the Gaussian spectral width.

A. Yield uncertainty

The uncertainty in the SRF-measured proton yield is largely dictated by the degree to which spectral modeling is required to infer the incident proton yield. For incident spectra where the thinnest filter comfortably transmits the entire spectrum, the yield uncertainty is limited by counting statistics in the CR-39 (typically ~±1% for protons at a fluence of 10^4/cm^2 over the ~cm^2 area covered by each window) and by uncertainties in background subtraction and discriminating proton tracks from background in the CR-39, typically ~3%. Particle fluence anisotropies can also contribute an additional uncertainty to the overall measured yield uncertainty, but these can be minimized in an appropriately-designed implosion where the protons are emitted $\gtrsim$ns after the end of the laser pulse.[18] The condition for a modeling-independent determination of the yield is—conservatively, greater than 99.9% of the proton spectrum transmitted through the 10-μm Ta filter for the "thick" SRF—is satisfied when, for example, $E_0 > 1.81$ MeV for $\sigma < 0.12$ MeV or when $E_0 > 2.35$ MeV for $\sigma < 0.34$ MeV (spectral widths chosen to span those observed on LEIA, OMEGA, and NIF). These conditions are illustrated in part in Figure 10, which shows the simulated proton transmission (or signal) through the different filters of the "thick" SRF. For the "thin" SRF, >99.9% of the proton spectrum is transmitted through the 5-μm filter when, e.g., $E_0 > 1.23$ MeV for $\sigma < 0.12$ MeV or when $E_0 > 1.90$ MeV for $\sigma < 0.34$ MeV. These energy ranges for 100% proton transmission through the thinnest filters are consistent with the analysis of SRF data from the LEIA and OMEGA experiments.

The N130129 data are an example of a spectrum where modeling is required to infer the incident proton yield, as a fraction of the spectrum was ranged out even in the thinnest (10-μm Ta) filter. In that case, uncertainty in the modeling itself contributes to the overall yield uncertainty. The objective of the modeling is to determine what fraction of the proton spectrum is detected and, thus, to correct for the fraction of protons that is ranged out. With a perfect understanding of the ranging process through the filters, this uncertainty would be negligible. However, uncertainty in the filter thickness, conservatively ± 1 μm for each individually-measured filter, contributes to the uncertainty in the modeled ratio of yield through the 10-μm filter to the actual yield (Y_{10}/Y_{actual}). The actual yield is inferred based on the measured Y_{10} and the modeling-inferred Y_{actual}/Y_{10} ratio, which is constrained by the measured signal ratios S_{14}/S_{10}, S_{19}/S_{10}, and S_{23}/S_{10}. In the case of N130129, adding 1 μm to the thickness of the 10-μm filter only slightly changes the relative signal ratios (S_{14}/S_{10} from 0.71 to 0.74, versus measured 0.71; S_{19}/S_{10} from 0.13 to 0.13, versus measured 0.13; S_{23}/S_{10} from 0.008 to 0.008, versus measured 0.014), while Y_{10}/Y_{actual} decreases from 0.97 to 0.93. Similarly, removing 1 μm from the thickness of the 10-μm filter only slightly changes the relative

signal ratios (S_{14}/S_{10} from 0.71 to 0.70, versus measured 0.71; S_{19}/S_{10} from 0.13 to 0.13, versus measured 0.13; S_{23}/S_{10} from 0.008 to 0.008, versus measured 0.014), while Y_{10}/Y_{actual} increases from 0.97 to 0.99. Therefore, this change to the modeling based on the bounds of measurement uncertainty of the filter thickness causes a barely-perceptible shift in the modeled signal ratios, but produces a ±3% change in the inferred yield. The uncertainty in the inferred yield resulting from uncertainties in the modeling must be addressed on a case-by-case basis, but should be no greater than of order ±4%–8%. This uncertainty is added in quadrature to the uncertainties in proton track counting as discussed above, for a total yield uncertainty of ±5%–10%.

B. Energy uncertainty

The ability to infer a mean proton energy likewise depends on the proton energy relative to the proton range in the different filters. When all protons are transmitted through the different filters (and the relative signal ratios are all 1), only a lower limit on the mean proton energy can be established, as was the case in the OMEGA data. A conservative upper limit on the energy range at which the mean energy can be determined is set by the energy at which a detectable loss of transmission can be observed through the thickest filter in the SRF, either 23 μm Ta for the current "thick" version or 20 μm Ta for the "thin" version. For purposes of this study, a detectable loss of transmission is considered to be below 97% of the protons transmitted (allowing for 3% uncertainty in the measured signal behind each filter). For the thick SRF, 97% transmission through 23 μm Ta is achieved when, e.g., $E_0 = 3.18$ MeV for $\sigma < 0.12$ MeV (Figure 10(a)) or when $E_0 = 3.57$ MeV for $\sigma < 0.34$ MeV (Figure 10(c)). The LEIA data shown in Figure 4(a), at a mean energy of $E_0 = 3.04$ MeV, is an example that is coming close to the limit below which a mean energy can be precisely inferred. For energies above these values, it is impossible to determine the exact mean energy. For the thin SRF, 97% transmission through 20 μm Ta is achieved when, e.g., $E_0 = 2.82$ MeV for $\sigma < 0.12$ MeV or when $E_0 = 3.23$ MeV for $\sigma < 0.34$ MeV. The OMEGA data shown in Figure 6 are all above this energy limit and, thus, the most information that can be inferred is that the mean energy is >2.84 MeV (for $\sigma \lesssim 0.15$ MeV). The use of thicker filters can extend the range of energies at which an accurate energy measurement can be made (beyond simply establishing a lower limit). For those spectra where only one filter transmits less than 100% of the proton spectrum, there is a degeneracy in inferring two spectral quantities (mean energy and spectral width) from only one relative signal ratio. Under these conditions, the inferred mean energy can be constrained by reasonable bounds on the spectral width (if known) or by the energy at which the second thickest filter begins to range out a detectable fraction of the spectrum.

The mean proton energy measurement is well-constrained when one or more filters transmits a fraction of the proton spectrum. As shown in Figures 10(a) and 10(c), this condition is satisfied when the incident mean energy is ~1–3 MeV. This is evident in the LEIA data shown in Figures 4(b)–4(d), where incident proton energy differences of 100–200 keV cause differences in the relative signal ratios (S_{14}/S_{10} in particular) of 10%-20%, considerably larger than the uncertainty in proton track counting on the CR-39. This sensitivity is also illustrated by the slopes of the relative transmission (or signal) ratio curves in Figures 10(b) and 10(d). Thus, the random uncertainty in the analysis (inferring E_0 based on the relative signal ratio) based on the ±4% random uncertainty in the proton signal measurement is ~±30 keV. Allowing for up to a ±1 μm filter thickness uncertainty, the corresponding uncertainty in the E_0 inferred from the modeling is ~±110 keV. The total energy uncertainty is around ±120 keV,[29] of order the difference between the SBD-measured and SRF-inferred energy values as shown in Table II. This energy uncertainty is equivalent to an uncertainty of ~±4 mg/cm^2 in a total ρR measurement based on the energy downshift of the DD-proton spectrum.

C. Linewidth uncertainty

To simultaneously constrain both the mean proton energy and spectral width, it is necessary to have multiple filters in which a measurable fraction of the incident proton spectrum has been ranged out. When the proton energy is too high and only the thickest filter transmits a fraction of the proton spectrum, there is a degeneracy between the mean energy and spectral width, as alluded to above. Under those circumstances, the relative signal ratio is much more sensitive to the mean energy than to the spectral width, resulting in a well-constrained mean energy, while the spectral width is poorly constrained. Thus, a spectral width measurement is only possible for the "thick" SRF when $E_0 < 2.71$ MeV (based on <97% of protons transmitted through the 19-μm Ta filter for $\sigma = 0.12$ MeV, see Figure 10(a)) or for the "thin" SRF when $E_0 < 2.24$ MeV (based on <97% of protons transmitted through the 15-μm Ta filter for $\sigma = 0.12$ MeV). The spectral width is most accurately inferred when the spectrum is broad enough (typically for $\sigma > 0.12$ MeV) that there is significant overlap in energy space between the spectra ranged through different filters. This can also be understood as there being more than one window with a non-zero, non-unity fraction of the spectrum. If only one window at a time (and not the thickest filter) shows a non-zero, non-unity signal relative to the other windows, the spectral width can be constrained to $\sigma \lesssim 0.12$ MeV for the present designs with ~4-5-μm Ta filtering differences between windows. This narrow-spectrum condition was present in the LEIA data presented in Sec. III A. A different SRF design with more filters and less incremental filtering between windows could potentially be used to measure the linewidth of narrower spectra. A summary of the proton mean energy and spectral width bounds for SRF measurements of the proton yield, mean energy, and spectral width, for different values of the mean energy and spectral width, is presented in Table V.

When the proton spectrum is broad enough and sufficiently low in energy that signal behind multiple filters is a fraction of the number of incident protons (for example, in the N130129 data), the uncertainty in the inferred spectral width

TABLE V. Summary of proton mean energy and spectral width bounds for SRF measurement of the proton yield, mean energy E_0, and spectral width σ. These are based on the "thick" SRF, with filters consisting of 10 μm, 14 μm, 19 μm, and 23 μm Ta. The energy ranges for the "thin" SRF are slightly lower, as discussed in the text.

Observable	E_0 range (σ limit)	Comments on analysis
Yield	$1.81 < E_0 < 9$ MeV ($\sigma < 0.12$ MeV)	No modeling required
Yield	$1 < E_0 < 1.81$ MeV ($\sigma > 0.12$ MeV)	Inferred from modeling
Yield	$2.35 < E_0 < 9$ MeV ($\sigma < 0.34$ MeV)	No modeling required
Yield	$1 < E_0 < 2.35$ MeV ($\sigma > 0.34$ MeV)	Inferred from modeling
Mean energy (E_0)	$2.71 < E_0 < 3.18$ MeV ($\sigma < 0.12$ MeV)	Measurement possible, but E_0/σ degeneracy
Mean energy (E_0)	$1 < E_0 < 2.71$ MeV ($\sigma > 0.12$ MeV)	Measurement well constrained
Mean energy (E_0)	$3.10 < E_0 < 3.57$ MeV ($\sigma < 0.34$ MeV)	Measurement possible, but E_0/σ degeneracy
Mean energy (E_0)	$1 < E_0 < 3.10$ MeV ($\sigma > 0.34$ MeV)	Measurement well constrained
Spectral width (σ)	$1 < E_0 < 2.71$ MeV ($\sigma > 0.12$ MeV)	Measurement well constrained
Spectral width (σ)	$1 < E_0 < 3.10$ MeV ($\sigma > 0.34$ MeV)	Measurement well constrained

is based on the uncertainty in the relative signal ratios used to infer σ. As an illustrative example, the data from N130129 ($S_{14}/S_{10} = 0.71$, $S_{19}/S_{10} = 0.13$, $S_{23}/S_{10} = 0.014$) is analyzed to infer $E_0 = 2.05$ MeV and $\sigma = 0.34$ MeV, with modeled signal ratios of $S_{14}/S_{10} = 0.71$, $S_{19}/S_{10} = 0.13$, $S_{23}/S_{10} = 0.008$ (Sec. III B). If the modeled σ were changed to 0.37 MeV, the modeled signal ratios become $S_{14}/S_{10} = 0.70$, $S_{19}/S_{10} = 0.15$, $S_{23}/S_{10} = 0.014$. Conversely, for $\sigma = 0.31$ MeV, the modeled signal ratios become $S_{14}/S_{10} = 0.72$, $S_{19}/S_{10} = 0.11$, $S_{23}/S_{10} = 0.005$. Thus, a 0.03 MeV difference on top of $\sigma = 0.34$ MeV corresponds to a ~15% departure for S_{19}/S_{10} and a ~50% difference in S_{23}/S_{10}. These differences are well outside of the uncertainty of the raw proton signal measurement, which are typically around ±4%. Therefore, a reasonable, conservative estimate of the uncertainty in the spectral width under such conditions is ~±30 keV. The approximate uncertainty in σ based on this kind of analysis is shown in Figure 11. The uncertainty in σ is inferred as the variation in the modeled σ that produces a ±0.03 change in any of the modeled signal ratios (S_{14}/S_{10}, S_{19}/S_{10}, and S_{23}/S_{10}). This analysis represents the maximum difference in σ that produces a non-observable (within measured signal uncertainties) change in the signal ratios. The ±0.03 variation is based on a ±4% uncertainty on a signal ratio of 0.70. In some cases

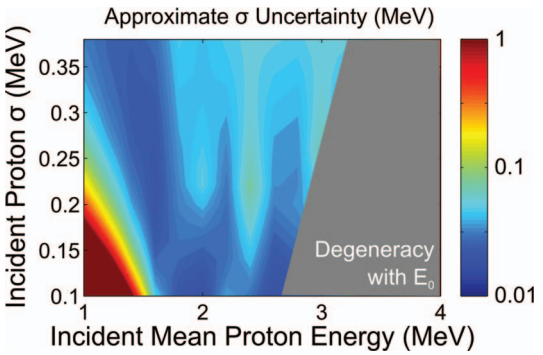

FIG. 11. Approximate uncertainty in the inferred σ using the thick SRF as a function of incident proton mean energy and σ. This uncertainty calculation is based on the variation in the modeled σ that produces a maximum variation of ±0.03 in any of the modeled proton signal ratios (S_{14}/S_{10}, S_{19}/S_{10}, and S_{23}/S_{10}). In the grey region, there is a degeneracy between the inferred E_0 and σ, so that the linewidth cannot be uniquely inferred.

where the signal ratios are much smaller, such as for S_{19}/S_{10} and S_{23}/S_{10} on shot N130129, the ±0.03 allowed variation is an extremely conservative condition. Typical uncertainty in σ based on this condition over the energy range of interest is ~±20-60 keV. Uncertainty in the filter thickness primarily translates to an uncertainty in the mean energy and does not substantially contribute to uncertainty in the inferred spectral width.

D. Uncertainty summary

The uncertainty in the mean energy and spectral width due to the uncertainty in the measured signal ratios can also be constrained simultaneously using a χ^2 analysis. Sweeping simultaneously the modeled mean energy and spectral width, the difference between measured signal ratios for the example of shot N130129 (S_{14}/S_{10}, S_{19}/S_{10}, and S_{23}/S_{10}) and their modeled counterparts ($S_{14}/S_{10,\,modeled}$, $S_{19}/S_{10,\,modeled}$, and $S_{23}/S_{10,\,modeled}$) has been computed. These differences have been normalized by an uncertainty in each signal ratio ($\Delta_{S14/S10} = 0.02$, $\Delta_{S19/S10} = 0.01$, $\Delta_{S23/S10} = 0.004$). These uncertainties have been chosen to correspond to the position-to-position variation in the different measurements, which is consistent also with the intrinsic ratio measurement uncertainty, though $\Delta_{S23/S10}$ was artificially enhanced to account for the increased modeling uncertainty for small S_{23}/S_{10} and low proton energy. Thus, the total χ^2 as a function of mean proton energy and linewidth has been calculated as

$$\chi^2(E_0,\sigma) = \frac{(S_{14}/S_{10,modeled}(E_0,\sigma) - S_{14}/S_{10})^2}{\Delta^2_{S14/S10}} + \frac{(S_{19}/S_{10,modeled}(E_0,\sigma) - S_{19}/S_{10})^2}{\Delta^2_{S19/S10}} + \frac{(S_{23}/S_{10,modeled}(E_0,\sigma) - S_{23}/S_{10})^2}{\Delta^2_{S23/S10}}, \quad (2)$$

and is shown in Figure 12. The χ^2 has a minimum value of 1.16 in the range of $E_0 = 2.05$ MeV and $\sigma = 0.34$ MeV, the mean energy and linewidth as inferred in Sec. III B. The minimum χ^2 being close to unity is expected for a two-parameter fit to three signal-ratio measurements. Constraining the

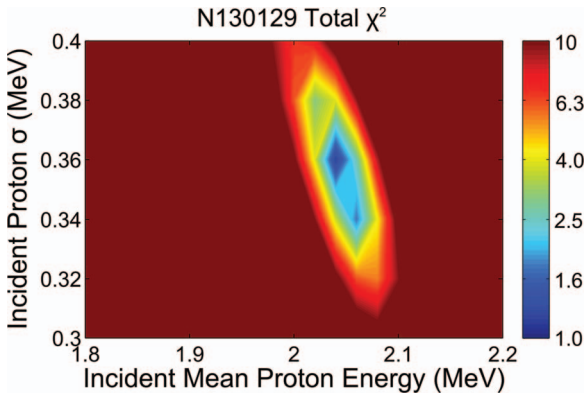

FIG. 12. Total χ^2 for analysis of SRF data from shot N130129, based on measured signal ratios of ($S_{14}/S_{10} = 0.71$, $S_{19}/S_{10} = 0.13$, $S_{23}/S_{10} = 0.014$) and measured signal-ratio uncertainties of $\Delta_{S14/S10} = 0.02$, $\Delta_{S19/S10} = 0.01$, $\Delta_{S23/S10} = 0.004$. This analysis allows for a simultaneous characterization of the mean energy and linewidth uncertainty resulting from uncertainty in the signal ratio measurements (based on variation in the signal ratios at different measurement positions, also allowing for additional uncertainty in S_{23}/S_{10} due to modeling difficulty at very low proton energy). As the minimum $\chi^2 = 1.16$, a doubling of χ^2 alows variation of ± 0.02 MeV in mean energy and ± 0.02 MeV in linewidth around the mean values of $E_0 = 2.05$ MeV and $\sigma = 0.34$ MeV.

uncertainty to be the variation in mean energy or linewidth that produces up to a factor of 2 increase in χ^2, an uncertainty of ± 0.02 MeV in mean energy and ± 0.02 MeV in linewidth is inferred. These mean energy and linewidth uncertainties due to the uncertainty in the measured signal ratios are in good agreement with those presented above and confirm the uncertainty quantification.

Thus, through different means, the optimal uncertainty in mean energy ($\sim\pm 0.03$ MeV) and linewidth ($\sim\pm 0.03$ MeV) as a result of uncertainty in the raw signal ratio measurements have been inferred, using the example of shot N130129. In addition, the uncertainty in the filter thickness contributes a ± 0.11 MeV uncertainty in the mean energy, for a total uncertainty under typical analysis conditions of ± 0.12 MeV. Degeneracy between mean energy and linewidth impacting a single signal ratio will increase the mean energy uncertainty and, especially, the linewidth uncertainty under certain conditions. When the linewidth measurement is well constrained, it can be evaluated with an uncertainty of $\pm$20–60 keV. The uncertainty in the yield inferred from a given SRF measurement can be as little as $\pm 3\%$ when modeling is not required, and will generally be $\pm 5\%$–10%. These uncertainty calculations are based on the representative examples discussed herein, and in general should be computed on a case-by-case basis.

E. Comments on energy range

It has been established that the SRF operates effectively as a spectrometer for proton spectra in the range $\sim$1–3 MeV. This energy range is limited on the low end by the presence of "ablator" protons, which are accelerated to energies up to $\sim$1 MeV by electric fields in the corona of ICF implosions for a variety of shell materials.[30,31] The yield of these ablator protons is much higher than the fusion-generated proton yields, and thus ablator ions overwhelm the DD-proton signal if not properly filtered. Based on the OMEGA (NIF) data using the thin (thick) SRF, it is determined that for the laser drive conditions in those experiments, with an intensity of $\sim 10^{15}$ ($\sim 5 \times 10^{14}$) W/cm^2, the ablator protons were at low enough energies to be ranged out in the 5-μm (10-μm) Ta filter and, therefore, did not impact the detection of DD protons. If the SRF filtering were made thinner in an attempt to detect lower-energy protons, the ablator protons may be able to pass through the filters and wash out the fusion proton signal.

The energy upper-limit for SRF operation is dictated primarily by the thickest filtering. As CR-39 can detect protons at 100% efficiency up to $\sim$8 MeV, the upper energy limit for simply detecting protons is the maximum incident energy of a proton such that, when ranged through the thickest SRF filter, it emerges on the CR-39 at an energy no greater than $\sim$8 MeV. For the current SRF configurations, with thickest filters of 20 μm and 23 μm Ta, that energy upper limit for detecting protons and measuring a proton yield is $\sim$9 MeV. As discussed above, this energy limit is not the same as that for spectroscopy, which relies on a differential in proton signal behind different filters; for the current configurations, the upper limit for measuring the mean proton energy is $\sim$3 MeV. In principle, both of these energy upper-limits can be increased by the use of additional or thicker filters.

V. CONCLUSIONS AND APPLICATIONS

A compact SRF proton spectrometer has been designed and implemented at OMEGA and the NIF for a yield, mean energy, and spectral width determination for the DD-proton spectrum in the energy range $\sim$1–3 MeV. Unlike other low-energy proton spectrometers used on ICF facilities, the SRF is highly portable and can be fielded at multiple positions around the implosion inside the target chamber. This instrument is a lower-energy analogue of the well-established WRF proton spectrometer, which operates in the energy range of 4–20 MeV. The SRF has been tested on LEIA and in implosions at OMEGA and the NIF. These experiments have demonstrated the sensitivity of the detector response to the mean proton energy and width of the incident spectrum. For a proton spectrum with a mean energy $E_0 < 3$ MeV, a typical uncertainty in the mean energy is $\sim\pm 0.12$ MeV. For a sufficiently broad spectrum ($\sigma > 0.12$ MeV) at a mean energy $<$2.7 MeV, the spectral width can be estimated with an uncertainty of $\sim\pm$30-50 keV.

The SRF was designed for diagnosis of thin-glass-shell ICF implosions ($<$30 mg/cm^2) with deuterium in the fuel (either D_2 or D^3He gas), which produce DD protons at a birth energy of $\sim$3.02 MeV. Measurements of the DD fusion yield and spectral width provide information about the ion temperature in the implosion, while the energy downshift is proportional to the areal density (up to a ρR of $\sim$30 mg/cm^2, at which point the DD protons are ranged out). This technique can be extended to higher energy ranges through the use of thicker filtering. The SRF could be of great value at the NIF for an *in situ* calibration of DD-neutron detectors.[17,18,28] With an appropriate change in filtering, the SRF can also be applied to the detection of D^3He- or DT-α particles in the energy range of 1-4 MeV. On D^3He-filled implosions, a second piece of

CR-39 placed behind the first and filtered appropriately can be used to simultaneously detect D^3He protons. The SRF can also be adapted for measurement of the $^3He^3He$-proton spectrum in fundamental nuclear science experiments.

ACKNOWLEDGMENTS

The authors thank the OMEGA and NIF operations and target fabrication crews for their assistance in carrying out these experiments and R. Frankel, E. Doeg, M. Valadez, M. Cairel, and M. McKernan for their help in processing of CR-39 data used in this work. The authors also thank G. Grim (LANL) for access to two OMEGA shots. This work was performed in partial fulfillment of the first author's Ph.D. thesis and supported in part by US DoE (Grant No. DE-NA0001857), NLUF (Grant No. DE-NA0002035), LLE (Grant No. 415935-G), LLNL (Grant No. B600100), and FSC (Grant No. 5-24431).

[1]Y. Kitagawa, K. Tanaka, M. Nakai, T. Yamanaka, K. Nishihara, H. Azechi, N. Miyanaga, T. Norimatsu, T. Kanabe, C. Chen *et al.*, Phys. Rev. Lett. **75**, 3130 (1995).
[2]C. K. Li, D. G. Hicks, F. H. Séguin, J. A. Frenje, R. D. Petrasso, J. M. Soures, P. B. Radha, V. Y. Glebov, C. Stoeckl, D. R. Harding, J. P. Knauer, R. Kremens, F. J. Marshall, D. D. Meyerhofer, S. Skupsky, S. Roberts, C. Sorce, T. C. Sangster, T. W. Phillips, M. D. Cable, and R. J. Leeper, Phys. Plasmas **7**, 2578 (2000).
[3]F. H. Séguin, C. K. Li, J. A. Frenje, D. G. Hicks, K. M. Green, S. Kurebayashi, R. D. Petrasso, J. M. Soures, D. D. Meyerhofer, V. Y. Glebov, P. B. Radha, C. Stoeckl, S. Roberts, C. Sorce, T. C. Sangster, T. W. Phillips, M. D. Cable, K. Fletcher, and S. Padalino, Phys. Plasmas **9**, 2725 (2002).
[4]R. D. Petrasso, J. A. Frenje, C. Li, F. H. Séguin, J. A. Frenje, J. R. Rygg, B. E. Schwartz, S. Kurebayashi, P. B. Radha, C. Stoeckl, J. M. Soures, J. Delettrez, V. Y. Glebov, D. D. Meyerhofer, and T. C. Sangster, Phys. Rev. Lett. **90**, 095002 (2003).
[5]D. G. Hicks, "Charged-particle spectroscopy: A new window on inertial confinement fusion," Ph.D. thesis (Massachusetts Institute of Technology, 1999).
[6]J. Cobble, K. Flippo, D. Offermann, F. Lopez, J. Oertel, D. Mastrosimone, S. Letzring, and N. Sinenian, Rev. Sci. Instrum. **82**, 113504 (2011).
[7]F. H. Séguin, J. A. Frenje, C. K. Li, D. G. Hicks, S. Kurebayashi, J. R. Rygg, B. E. Schwartz, R. D. Petrasso, S. Roberts, J. M. Soures, D. D. Meyerhofer, T. C. Sangster, J. P. Knauer, C. Sorce, V. Y. Glebov, C. Stoeckl, T. W. Phillips, R. J. Leeper, K. Fletcher, and S. Padalino, Rev. Sci. Instrum. **74**, 975 (2003).
[8]C. Freeman, G. Fiksel, C. Stoeckl, N. Sinenian, M. Canfield, G. Graeper, A. Lombardo, C. Stillman, S. Padalino, C. Mileham *et al.*, Rev. Sci. Instrum. **82**, 073301 (2011).
[9]R. L. Fleischer, P. B. Price, and R. M. Walker, J. Appl. Phys. **36**, 3645 (1965).
[10]K. Kinoshita and P. B. Price, Rev. Sci. Instrum. **51**, 32 (1980).
[11]G. Dajkó, Radiat. Prot. Dosim. **66**, 359 (1996).
[12]M. J. Rosenberg, F. H. Séguin, C. J. Waugh, H. G. Rinderknecht, D. Orozco, J. A. Frenje, M. G. Johnson, H. Sio, A. B. Zylstra, N. Sinenian, C. K. Li, R. D. Petrasso, V. Y. Glebov, C. Stoeckl, M. Hohenberger, T. C. Sangster, S. LePape, A. J. Mackinnon, R. M. Bionta, O. L. Landen, R. A. Zacharias, Y. Kim, H. W. Herrmann, and J. D. Kilkenny, Rev. Sci. Instrum. **85**, 043302 (2014).
[13]T. R. Boehly, D. L. Brown, R. S. Craxton, R. L. Keck, J. P. Knauer, J. H. Kelly, T. J. Kessler, S. A. Kumpan, S. J. Loucks, S. A. Letzring, F. J. Marshall, R. L. McCrory, S. F. B. Morse, W. Seka, J. M. Soures, and C. P. Verdon, Opt. Commun. **133**, 495 (1997).
[14]F. H. Séguin, N. Sinenian, M. Rosenberg, A. Zylstra, M. J.-E. Manuel, H. Sio, C. Waugh, H. G. Rinderknecht, M. G. Johnson, J. Frenje, C. K. Li, R. Petrasso, T. C. Sangster, and S. Roberts, Rev. Sci. Instrum. **83**, 10D908 (2012).
[15]G. Miller, E. Moses, and C. Wuest, Opt. Eng. **43**, 2841 (2004).
[16]M. J. Rosenberg *et al.*, "Utilization of NIF diagnostic development shots for investigation of ion kinetic effects in direct-drive exploding-pusher implosions," Phys. Plasmas (submitted).
[17]D. L. Bleuel, C. B. Yeamans, L. A. Bernstein, R. M. Bionta, J. A. Caggiano, D. T. Casey, G. W. Cooper, O. B. Drury, J. A. Frenje, C. A. Hagmann, R. Hatarik, J. P. Knauer, M. G. Johnson, K. M. Knittel, R. J. Leeper, J. M. McNaney, M. Moran, C. L. Ruiz, and D. H. G. Schneider, Rev. Sci. Instrum. **83**, 10D313 (2012).
[18]C. J. Waugh *et al.*, "A method for *in situ* absolute yield calibration of neutron time-of-flight detectors on OMEGA using CR-39-based proton detectors," Rev. Sci. Instrum. (unpublished).
[19]N. Sinenian, M. J.-E. Manuel, A. B. Zylstra, M. Rosenberg, C. J. Waugh, H. G. Rinderknecht, D. T. Casey, H. Sio, J. K. Ruszczynski, L. Zhou, M. G. Johnson, J. A. Frenje, F. H. Séguin, C. K. Li, R. D. Petrasso, C. L. Ruiz, and R. J. Leeper, Rev. Sci. Instrum. **83**, 043502 (2012).
[20]A. B. Zylstra, J. A. Frenje, F. H. Séguin, M. J. Rosenberg, H. G. Rinderknecht, M. G. Johnson, D. T. Casey, N. Sinenian, M. J.-E. Manuel, C. J. Waugh, H. W. Sio, C. K. Li, R. D. Petrasso, S. Friedrich, K. Knittel, R. Bionta, M. McKernan, D. Callahan, G. W. Collins, E. Dewald, T. Doppner, M. J. Edwards, S. Glenzer, D. G. Hicks, O. L. Landen, R. Lonson, A. Mackinnon, N. Meezan, R. R. Prasad, J. Ralph, M. Richardson, J. R. Rygg, S. Sepke, S. Weber, R. Zacharias, E. Moses, J. Kilkenny, A. Nikroo, T. C. Sangster, V. Glebov, C. Stoeckl, R. Olson, R. J. Leeper, J. Kline, G. Kyrala, and D. Wilson, Rev. Sci. Instrum. **83**, 10D901 (2012).
[21]Intrinsic background in the CR-39 consists of small defects which can appear to have similar characteristics as real proton tracks and must be discriminated away or subtracted out from the measured signal.
[22]J. F. Ziegler, M. D. Ziegler, and J. P. Biersack, Nucl. Instrum. Methods Phys. Res., Sect. B **268**, 1818 (2010).
[23]A. B. Zylstra, J. A. Frenje, F. H. Séguin, M. G. Johnson, D. T. Casey, M. J. Rosenberg, C. Waugh, N. Sinenian, M. J.-E. Manuel, C. K. Li, R. D. Petrasso, Y. Kim, and H. W. Herrmann, Nucl. Instrum. Methods Phys. Res., Sect. A **681**, 84 (2012).
[24]D. G. Hicks, C. K. Li, F. H. Séguin, A. K. Ram, J. A. Frenje, R. D. Petrasso, J. M. Soures, V. Y. Glebov, D. D. Meyerhofer, S. Roberts, C. Sorce, C. Stoeckl, T. C. Sangster, and T. W. Phillips, Phys. Plasmas **7**, 5106 (2000).
[25]S. Skupsky, J. A. Marozas, R. S. Craxton, R. Betti, T. J. B. Collins, J. A. Delettrez, V. N. Goncharov, P. W. McKenty, P. B. Radha, T. R. Boehly, J. P. Knauer, F. J. Marshall, D. R. Harding, J. D. Kilkenny, D. D. Meyerhofer, T. C. Sangster, and R. L. McCrory, Phys. Plasmas **11**, 2763 (2004).
[26]P. W. McKenty, R. S. Craxton, A. Shvydky, F. J. Marshall, R. L. McCrory, J. D. Kilkenny, A. Nikroo, M. L. Hoppe, A. J. Mackinnon, and M. J. Edwards, Bull. Am. Phys. Soc. **55**, 15 (2010).
[27]V. Y. Glebov, C. Stoeckl, T. C. Sangster, S. Roberts, G. J. Schmid, R. A. Lerche, and M. J. Moran, Rev. Sci. Instrum. **75**, 3559 (2004).
[28]V. Y. Glebov, D. D. Meyerhofer, T. C. Sangster, C. Stoeckl, S. Roberts, C. A. Barrera, J. R. Celeste, C. J. Cerjan, L. S. Dauffy, D. C. Eder, R. L. Griffith, S. W. Haan, B. A. Hammel, S. P. Hatchett, N. Izumi, J. R. Kimbrough, J. A. Koch, O. L. Landen, R. A. Lerche, B. J. MacGowan, M. J. Moran, E. W. Ng, T. W. Phillips, P. M. Song, R. Tommasini, B. K. Young, S. E. Caldwell, G. P. Grim, S. C. Evans, J. M. Mack, T. J. Sedillo, M. D. Wilke, D. C. Wilson, C. S. Young, D. Casey, J. A. Frenje, C. K. Li, R. D. Petrasso, F. H. Séguin, J. L. Bourgade, L. Disdier, M. Houry, I. Lantuejoul, O. Landoas, G. A. Chandler, G. W. Cooper, R. J. Leeper, R. E. Olson, C. L. Ruiz, M. A. Sweeney, S. P. Padalino, C. Horsfield, and B. A. Davis, Rev. Sci. Instrum. **77**, 10E715 (2006).
[29]This energy uncertainty is roughly comparable to that of the WRF proton spectrometer used at a higher energy range,[7,14,20] 4–20 MeV, in contrast to the ~1–3 MeV range for energy measurement using the present SRF spectrometer.
[30]D. G. Hicks, C. K. Li, F. H. Séguin, J. D. Schnittman, A. K. Ram, J. A. Frenje, R. D. Petrasso, J. M. Soures, D. D. Meyerhofer, S. Roberts, C. Sorce, C. Stoeckl, T. C. Sangster, and T. W. Phillips, Phys. Plasmas **8**, 606 (2001).
[31]N. Sinenian, A. B. Zylstra, M. J.-E. Manuel, H. G. Rinderknecht, J. A. Frenje, F. H. Séguin, C. K. Li, R. D. Petrasso, V. Goncharov, J. Delettrez, I. V. Igumenshchev, D. H. Froula, C. Stoeckl, T. C. Sangster, D. D. Meyerhofer, J. A. Cobble, and D. G. Hicks, Appl. Phys. Lett. **101**, 114102 (2012).